

# Creation and control of a two-dimensional electron liquid at the bare SrTiO<sub>3</sub> surface

W. Meevasana<sup>1,2,3,4,5\*</sup>, P.D.C. King<sup>3\*</sup>, R.H. He<sup>1,2</sup>, S.-K. Mo<sup>1,6</sup>, M. Hashimoto<sup>1,6</sup>,

A. Tamai<sup>3</sup>, P. Songsiriritthigul<sup>4,5</sup>, F. Baumberger<sup>3</sup>, Z.-X. Shen<sup>1,2§</sup>

<sup>1</sup>*Departments of Physics and Applied Physics,  
Stanford University, CA 94305, USA*

<sup>2</sup>*Stanford Institute for Materials and Energy Sciences,  
SLAC National Accelerator Laboratory,  
2575 Sand Hill Road, Menlo Park, CA 94025, USA*

<sup>3</sup>*School of Physics and Astronomy,  
University of St Andrews, North Haugh,  
St. Andrews, Fife KY16 9SS, UK*

<sup>4</sup>*School of Physics, Suranaree University of  
Technology and Synchrotron Light Research Institute,  
Nakhon Ratchasima, 30000, Thailand*

<sup>5</sup>*Thailand Center of Excellence in Physics, CHE, Bangkok, 10400, Thailand*

<sup>6</sup>*Advanced Light Source, Lawrence Berkeley National Lab, Berkeley, CA 94720, USA*

*\*These authors contributed equally to this work. and*

*§To whom correspondence should be addressed; E-mail: zxshen@stanford.edu*

(Dated: May 23, 2018)

Many-body interactions in transition-metal oxides give rise to a wide range of functional properties, such as high-temperature superconductivity [1], colossal magnetoresistance [2], or multiferroicity [3]. The seminal recent discovery of a two-dimensional electron gas (2DEG) at the interface of the insulating oxides  $\text{LaAlO}_3$  and  $\text{SrTiO}_3$  [4] represents an important milestone towards exploiting such properties in all-oxide devices [5]. This conducting interface shows a number of appealing properties, including a high electron mobility [4, 6], superconductivity [7], and large magnetoresistance [8] and can be patterned on the few-nanometer length scale. However, the microscopic origin of the interface 2DEG is poorly understood. Here, we show that a similar 2DEG, with an electron density as large as  $8 \times 10^{13} \text{ cm}^{-2}$ , can be formed at the bare  $\text{SrTiO}_3$  surface. Furthermore, we find that the 2DEG density can be controlled through exposure of the surface to intense ultraviolet (UV) light. Subsequent angle-resolved photoemission spectroscopy (ARPES) measurements reveal an unusual coexistence of a light quasiparticle mass and signatures of strong many-body interactions.

It has been known for decades that strong electron correlations in oxide materials give rise to a rich variety of electronic phases, which are highly susceptible to small changes of control parameters. Although this situation is ideal for applications, the potential of all-oxide electronic devices had been questioned until very recently. Indeed, it was thought that the chemical complexity of most oxides would yield devices much inferior to those based on conventional semiconductors [5]. A paradigm-shift came when Ohtomo and Hwang demonstrated unprecedented control of the complex  $\text{LaAlO}_3/\text{SrTiO}_3$  interface [4], leading to the formation of a high-mobility electron gas [6]. The carrier density and sheet conductivity of the interface 2DEG react sensitively to gate fields and it was successfully patterned on the nano-scale [9], which is central to the development of oxide electronics [10]. However, a full understanding of the origin of this 2DEG remains elusive. The two main contenders are oxygen vacancies at the interface [11, 12], and an electronic reconstruction to avoid a polar-catastrophe [4, 13]. Distinguishing between these mechanisms is an essential step in the development of a new generation of all-oxide devices.

In this letter, we show that a similar 2DEG can be created at the bare, unreconstructed  $\text{SrTiO}_3$  surface. Furthermore, we demonstrate control of its carrier density through exposure to intense UV radiation. Fig. 1 shows ARPES data from the cleaved (001) surface

of 0.1% La-doped SrTiO<sub>3</sub>(001) following exposure to UV synchrotron light. At least two electron-like band dispersions can be observed from the ARPES data (Fig. 1a,b). The shallower band, with Fermi wave number  $k_F = 0.12 \text{ \AA}^{-1}$ , and deeper band, with  $k_F = 0.175 \text{ \AA}^{-1}$ , have their band bottoms situated  $\sim 110$  and  $216$  meV below the Fermi level, respectively. We have investigated the dimensionality of the induced electronic system by varying the photon energy, and thus probing the band dispersion along  $k_z$  (surface normal). Fig. S2 (supplementary information) shows that the states have negligible dispersion along  $k_z$ . This is the defining property of a two-dimensional electronic state whose wavefunction is confined along the  $z$ -direction to a layer of comparable thickness to the Fermi wavelength. Also, these bands cannot be associated with the bulk electronic structure: the photon energy used to record the data shown in Fig. 1 corresponds to  $k_z$  of approximately  $3.2\pi/a$  [14], close to the Brillouin zone boundary where no bulk bands exist in the vicinity of the Fermi energy, even for samples with more than an order of magnitude higher bulk carrier density than those measured here. Consequently, we attribute these states to a surface 2DEG.

In order to obtain the surface charge density, we extract the Luttinger area from the Fermi surface map shown in Fig. 1(c). Two concentric Fermi surface sheets are observed, corresponding to the two dispersions in Fig. 1(a). The intensity variation across the measured Fermi surface is due to pronounced matrix element effects. The charge density  $n_{2D}$  from each concentric sheet can then be estimated by  $n_{2D} = k_F^2/2\pi$ , allowing the total surface charge density to be determined as  $7.1 \pm 2 \times 10^{13} \text{ cm}^{-2}$ . This value falls within the range of the 2DEG densities observed at LaAlO<sub>3</sub>/SrTiO<sub>3</sub> interfaces [7, 11, 12]. The effective masses extracted from parabolic fits to the two measured dispersions (Fig. 1a) yield surprisingly low values of  $0.5 - 0.6 m_e$ , substantially lower than the bulk band masses. This will contribute to the high electron mobility [4].

Furthermore, as shown in Fig. 2, we find that the 2DEG density is not fixed to one particular value, but can be varied by exposure of the cleaved surface to different irradiation doses of UV light. We found no evidence of any 2DEG states from initial ARPES measurements of the freshly cleaved surface, suggesting that the 2DEG only forms after exposure to UV light. Following exposure to 55 eV UV light for an irradiation dose of  $\sim 32 \text{ J/cm}^2$  (Fig. 2a), we observe a single shallow band with  $k_F \sim 0.1 \text{ \AA}^{-1}$  and a band bottom  $\sim 60$  meV below  $E_F$ . Upon increasing the irradiation dose, this band moves downwards, to higher binding energies, with a second band becoming visible between the first band and the Fermi

level. The  $k_F$  positions and occupied bandwidth of these two bands continue to increase slowly with further increase in irradiation dose. The corresponding surface charge densities extracted from the measured bands are plotted in Fig. 2f, revealing a monotonic increase in 2DEG density with increasing irradiation dose. Therefore, the method utilised here provides a controllable means with which to modify the 2DEG density.

We note that Fig. 2g and 2h, which are measured immediately after Fig. 2b and 2e, respectively, but with lower intensity of the probing beam ( $I = 0.06 \text{ W/cm}^2$ ), show identical band dispersions within experimental accuracy. Similar results have been obtained for spectra taken up to an hour after irradiation with an intense UV beam (not shown). This demonstrates that the 2DEG reported here is a ground state property of the UV-irradiated SrTiO<sub>3</sub> surface. Hence, its origin must be fundamentally different from photocarrier doping effects, which have characteristic lifetimes of the excited states  $< 1 \text{ ms}$  at low temperature [15].

It is clear, therefore, that the irradiation by UV light mediates a change in the surface of the SrTiO<sub>3</sub>, which consequently induces the 2DEG. Clear  $(1 \times 1)$  low-energy electron diffraction (LEED) patterns observed both before and after the UV exposure indicate that the surface does not reconstruct during this process (see Supplementary Fig. S1). Therefore, creation of a surface 2DEG brought about by a change in the intrinsic surface state distribution due to surface reconstruction can be ruled out. This indicates that extrinsic states, such as donor-like defects or adsorbates, induce the 2DEG. In particular, oxygen vacancies localized at the surface would be expected to lead to a surface electron accumulation, with charge neutrality requiring the creation of an electron 2DEG to screen the positive surface charge of such ionized defect centres. Experimental studies on LaAlO<sub>3</sub>/SrTiO<sub>3</sub> interfaces [11, 12] have shown that oxygen vacancies can be created during the sample preparation process under low oxygen pressures. Here, we suggest that exposure to intense UV light in ultra-high vacuum causes oxygen desorption from the surface. Such a photon-induced chemical change was previously observed in photoluminescence spectra of SrTiO<sub>3</sub> following irradiation with 325nm laser light [16], where a sub-band-gap luminescence peak, growing in magnitude with increasing irradiation, and stable for some time following the irradiation, was assigned to photo-induced oxygen vacancies. This is consistent with an increased in-gap defect state [17] that we observe at  $\sim 1.3\text{eV}$  below the Fermi level in angle-integrated photoemission spectra following the UV exposure (see Supplementary Information).

We cannot exclude that this in-gap state could also arise from adsorbed impurities such as hydrogen, which could themselves provide the required donor-type surface states, as discussed in the supplementary information. However, irrespective of the exact microscopic identification of the defects causing the charge accumulation, the results presented above demonstrate that it is not necessary to have an interface with the polar surface of another material in order to obtain a 2DEG at the surface of SrTiO<sub>3</sub>. Indeed, we find that extrinsic mechanisms are sufficient to induce a ground-state 2DEG of the same density. Apart from obvious advantages for their spectroscopic investigation, the methodology employed here to create such a 2DEG offers potential for the realization of novel schemes in oxide electronics. While existing approaches have the ability to pattern the spatial extent of the LaAlO<sub>3</sub>/SrTiO<sub>3</sub> interface 2DEG [9, 18], our work opens the way to spatial control of its ground state density by employing focussed light. Furthermore, UV interference patterns could be employed to allow much faster parallel nano-scale patterning of the 2DEG. This should not be specific to the surface of SrTiO<sub>3</sub>, and could be employed for creation of surface 2DEGs across a range of oxide materials. The scheme should also be useful to write surface charge on LaAlO<sub>3</sub> by desorbing oxygen. For a thin layer of LaAlO<sub>3</sub> grown on SrTiO<sub>3</sub>, charge localized at the surface of the LaAlO<sub>3</sub> is thought to provide the mechanism for writing of metallic lines at the LaAlO<sub>3</sub>/SrTiO<sub>3</sub> interface using conducting atomic-force microscopy [19]. Writing of surface charge on the LaAlO<sub>3</sub> layer using UV interference patterns could therefore be an attractive route towards efficient processing of a high-mobility modulation-doped 2DEG, patterned at the nano-scale.

To further characterize the 2DEG created here, we adapt a model originally developed for conventional semiconductors [20]. The charge resulting from surface- (or indeed interface-) localised oxygen vacancies induces a spatial redistribution of bulk carriers in the vicinity of the surface/interface, correlated with a bending of the electronic bands relative to the Fermi level. If the potential well created by this band bending is sufficiently deep, it causes the conduction band states to become quantized into two-dimensional (2D) subbands. We have performed coupled Poisson-Schrödinger calculations [20] for such a band-bending scenario. Incorporating an electric-field dependence of the susceptibility [21] within our model, we find that the downward band bending in SrTiO<sub>3</sub> (Fig. 3b) is indeed very rapid. This leads to a narrow 2DEG (Fig. 3c) in a 3D crystal due only to the strength of the internal electric field. Its lowest subband is localized within  $\approx 4$  unit cells from the surface and is followed by a

series of higher subbands with wavefunctions that progressively extend deeper into the bulk (see Supplementary Fig. S4). As shown in Fig. 3a, these subbands effectively reproduce the two main dispersions observed in the ARPES data, confirming that the states observed here can broadly be described as the quantum well states of a surface 2DEG resulting from a downward band bending. The additional weakly bound states found in the calculations at lower binding energies are not resolved experimentally. This is possibly due to low matrix elements for shallow quantum well states, which generally have small amplitudes of the wave function in the near-surface region probed by ARPES, as shown in Supplementary Fig. S4. Further, since the wave functions of these shallow states expand over a much larger depth than the more localized deeper states, the shallow states might start dispersing in  $k_z$ , causing them to become smeared out in the ARPES measurements, possibly beyond our detection limit.

Our model does not take intra-unit cell potential variations into account, thought to be important for the relatively local Ti 3d states. Nonetheless, it is in good qualitative agreement with density-functional theory calculations for the LaAlO<sub>3</sub>/SrTiO<sub>3</sub> interface by Popović *et al.* [22], which report a similar reconstruction of the electronic structure in the 2DEG into a ladder of subbands. The lowest of these was identified as an in-plane Ti  $d_{xy}$  state largely localized on the interfacial TiO<sub>2</sub> layer, whereas the charge density from a series of higher-lying  $d_{xy}$  states appeared spread out over several layers in the calculation. Additionally these authors found  $d_{yz}$  and  $d_{xz}$  derived states with strongly elliptical Fermi surfaces and high effective masses for transport along  $x$  and  $y$ , respectively. In the present case, we observe only two concentric isotropic Fermi surfaces of light carriers, which we attribute to the lowest members of a ladder of  $d_{xy}$  states. However, we cannot rule out the additional presence of heavy  $d_{xz/yz}$  bands in the surface 2DEG, since their intensity would be suppressed relative to  $d_{xy}$  states in the experimental geometry and polarization employed here. Also, the Fermi level in our experiment lies closer to the lowest subband minimum than in the calculations of Popović *et al.* [22] for the LaAlO<sub>3</sub>/SrTiO<sub>3</sub> interface, and so the  $d_{xz/yz}$  states, if present, should be quite shallow and hence extend deep in the bulk, which would reduce their intensity in ARPES.

Although most conventional semiconductors exhibit a depletion of charge carriers at the surface, a small number have themselves been observed to support a surface 2DEG, concomitant with a downward band bending [23]. Comparing the 2DEG states from one

such example, InAs [24] shown in Fig. 4b, with those of SrTiO<sub>3</sub> observed here (Fig. 4a), reveals a qualitative similarity between the two materials. This further confirms the validity of the above model. However, some important differences are also apparent. In particular, there is pronounced spectral weight in SrTiO<sub>3</sub> at binding energies much higher than the band bottom. This effect is absent for the semiconductor case, but can be seen in ARPES measurements of other strongly-correlated compounds such as the cuprate high-temperature superconductor Bi<sub>2</sub>Sr<sub>2</sub>CuO<sub>6</sub> (Fig. 4c) [26]. The non-vanishing spectral weight in SrTiO<sub>3</sub> implies a finite electron self-energy at high binding energies, giving direct evidence of enhanced many-body interactions inherent to the 2DEG states of SrTiO<sub>3</sub>. Hence, the 2DEG here is best described as an electron liquid rather than an electron gas [27]. Besides this spectral weight below the band bottom, we also note that the SrTiO<sub>3</sub> data show weak dispersion anomalies (kinks) at a binding energy around 20-30 meV and, less clearly, around 70-80 meV below the Fermi level, which we assign to electron-phonon interactions with a weaker coupling strength than observed in the bulk [14].

In systems where electronic correlations play an important role, the quasiparticles are normally found to be heavy. Intriguingly, however, the strong electron correlations we observe here do not lead to a substantial mass enhancement within the 2DEG. In fact, the effective mass of 0.5-0.6m<sub>e</sub> extracted from the data is lower than the lightest bulk band mass of ~m<sub>e</sub> estimated from ref. [14]. Almost certainly, this will apply to the LaAlO<sub>3</sub>/SrTiO<sub>3</sub> interface 2DEG too, which helps to explain the high electron mobilities achieved in this system. While a direct spectroscopic measurement of the electronic band dispersion within the 2DEG, as performed here, has not yet been achieved in the interface systems, this conclusion is supported by very recent measurements of the penetration field in front-gated LaAlO<sub>3</sub>/SrTiO<sub>3</sub> heterostructures, where a 2DEG band mass significantly below any of the bulk masses was inferred [28]. We speculate that this unusual behaviour might be due to an interaction-induced shrinkage of the fundamental band gap approaching the surface of SrTiO<sub>3</sub> [24]. This would effectively increase the depth of the potential well and hence result in steeper quantized bands/lighter band masses. If this picture is true, the surface of SrTiO<sub>3</sub>, or indeed its interface with LaAlO<sub>3</sub>, are rare examples where many-body interactions have the counter-intuitive effect of increasing the mobility. A full understanding of this will require further theoretical and experimental studies. Spectroscopic investigations of surface 2DEGs, of the form reported here, will likely prove essential to elucidate the fundamental

electronic structure and underlying role of many-body interactions in oxide 2DEGs, and so will play a major role in the development of all-oxide electronics.

- 
- [1] Bednorz, J.G. & Muller, K.A. Perovskite-type oxides: The new approach to high-Tc superconductivity. *Rev. Mod. Phys.* **60**, 585-600 (1988).
  - [2] Von Helmolt, R. *et al.* Giant negative magnetoresistance in perovskitelike  $\text{La}_{2/3}\text{Ba}_{1/3}\text{MnO}_x$  ferromagnetic films. *Phys. Rev. Lett.* **71**, 2331-2333 (1993).
  - [3] Kimura, T. *et al.* Magnetic control of ferroelectric polarization. *Nature* **426**, 55-58 (2003).
  - [4] Ohtomo, A. & Hwang, H.Y. A high-mobility electron gas at the  $\text{LaAlO}_3/\text{SrTiO}_3$  heterointerface. *Nature* **427**, 423-426 (2004).
  - [5] Takagi, H. & Hwang, H.Y. An Emergent Change of Phase for Electronics. *Science* **327**, 1601-1602 (2010).
  - [6] Thiel, S. *et al.*, Tunable Quasi-Two-Dimensional Electron Gases in Oxide Heterostructures. *Science* **313**, 1942-1945 (2006).
  - [7] Reyren, N. *et al.*, Superconducting Interfaces Between Insulating Oxides. *Science* **317**, 1196-1199 (2007).
  - [8] Brinkman, A. *et al.* Magnetic effects at the interface between non-magnetic oxides. *Nature Mater.* **6**, 493-496 (2007).
  - [9] Cen, C. *et al.* Nanoscale control of an interfacial metal-insulator transition at room temperature. *Nature Mater.* **7**, 298-302 (2008).
  - [10] Mannhart, J. & Scholm, D. G. Oxide Interfaces — An Opportunity for Electronics. *Science* **327**, 1607-1611 (2010).
  - [11] Siemons, W. *et al.* Origin of Charge Density at  $\text{LaAlO}_3$  on  $\text{SrTiO}_3$  Heterointerfaces: Possibility of Intrinsic Doping. *Phys. Rev. Lett.* **98**, 196802 (2007).
  - [12] Kalabukhov, A. *et al.* Effect of oxygen vacancies in the  $\text{SrTiO}_3$  substrate on the electrical properties of the  $\text{LaAlO}_3/\text{SrTiO}_3$  interface. *Phys. Rev. B* **75**, 121404(R) (2007).
  - [13] Nakagawa, N., Hwang, H. Y. & Muller, D. A. Why some interfaces cannot be sharp. *Nature Mater.* **5**, 204-209 (2006).
  - [14] Meevasana, W. *et al.* Strong energy-momentum dispersion of phonon-dressed carriers in the lightly doped band insulator  $\text{SrTiO}_3$ . *New. J. Phys.* **12**, 023004 (2010).

- [15] Kozuka, Y. *et al.* Optically tuned dimensionality crossover in photocarrier-doped SrTiO<sub>3</sub>: Onset of weak localization. *Phys. Rev. B* **76**, 085129 (2007).
- [16] Mochizuki, S. *et al.* Photoluminescence and reversible photo-induced spectral change of SrTiO<sub>3</sub>. *J. Phys.:Condens. Matter* **17**, 923-948 (2005).
- [17] Aiura, Y. *et al.* Photoemission study of the metallic state of lightly electron-doped SrTiO<sub>3</sub>. *Surf. Sci.* **515**, 61-74 (2002), *and references therein.*
- [18] Caviglia, A. D. *et al.* Electric field control of the LaAlO<sub>3</sub>/SrTiO<sub>3</sub> interface ground state. *Nature* **456**, 624-627 (2008).
- [19] Xie, Y. *et al.* Charge Writing at the LaAlO<sub>3</sub>/SrTiO<sub>3</sub> Surface. *Nano Lett.* **10**, 2588-2591 (2010).
- [20] King, P. D. C., Veal, T. D. & McConville, C. F. Non-parabolic coupled Poisson-Schrodinger solutions for quantized electron accumulation layers: Band bending, charge profile, and subbands at InN surfaces. *Phys. Rev. B* **77**, 125305 (2008).
- [21] Copie, O. *et al.* Towards Two-Dimensional Metallic Behavior at LaAlO<sub>3</sub>/SrTiO<sub>3</sub> Interfaces. *Phys. Rev. Lett.* **102**, 216804 (2009).
- [22] Popović, Z. S., Satpathy, S. & Martin, R. M. Origin of the Two-Dimensional Electron Gas Carrier Density at the LaAlO<sub>3</sub> or SrTiO<sub>3</sub> interface. *Phys. Rev. Lett.* **101**, 256801 (2008).
- [23] King, P.D.C. *et al.*, Surface Electron Accumulation and the Charge Neutrality Level in In<sub>2</sub>O<sub>3</sub>. *Phys. Rev. Lett.* **101**, 116808 (2008), *and references therein.*
- [24] King, P. D. C. *et al.* Surface band gap narrowing in quantized electron accumulation layers. *Phys. Rev. Lett.* **104**, 256803 (2010).
- [25] Colakerol, L. *et al.* Quantized Electron Accumulation States in Indium Nitride Studied by Angle-Resolved Photoemission Spectroscopy. *Phys. Rev. Lett.* **97**, 237601 (2006).
- [26] Meevasana, W. *et al.* Hierarchy of multiple many-body interaction scales in high-temperature superconductors. *Phys. Rev. B* **75**, 174506 (2007).
- [27] Breitschaft, M. *et al.* Two-dimensional electron liquid state at LaAlO<sub>3</sub>-SrTiO<sub>3</sub> interfaces. *Phys. Rev. B* **81**, 153414 (2010).
- [28] Li, L. *et al.* Large capacitance enhancement and negative compressibility of two-dimensional electronic systems at LaAlO<sub>3</sub>/SrTiO<sub>3</sub> interfaces. Preprint at <<http://arxiv.org/pdf/1006.2847>> (2010).

## **Acknowledgments**

We would like to thank H.Y. Hwang, H. Takagi, M.R. Beasley, J. L. M. van Mechele, D. van der Marel, P. Reunchan, and S. Limpijumnong for helpful discussions. W.M. would like to thank H. Nakajima and Y. Rattanachai for help with the resistivity measurement. The work at ALS and Stanford Institute for Materials and Energy Sciences are supported by DOE's Office of Basic Energy Sciences under Contracts No. DE-AC02-76SF00515 and DE-AC03-76SF00098. The work at St Andrews is supported by the UK-EP SRC (EP/F006640/1) and the ERC (207901). W.M. acknowledges The Thailand Research Fund, Office of the Higher Education Commission and Suranaree University of Technology for financial support.

### **A. Author contributions**

ARPES measurements were performed by W.M., P.D.C.K., R.-H.H., F.B., and A.T. W.M. and P.D.C.K. analysed the ARPES data. W.M., P.D.C.K. and F.B. wrote the paper with suggestions and comments by R.-H.H., S.-K.M. and Z.-X.S. Calculations of quantized 2DEG states were done by P.D.C.K. S.-K.M. and M.H. maintained the ARPES endstation. Resistivity measurements were performed by W.M. and P.S. Z.-X.S. and F.B. are responsible for project direction, planning and infrastructure.

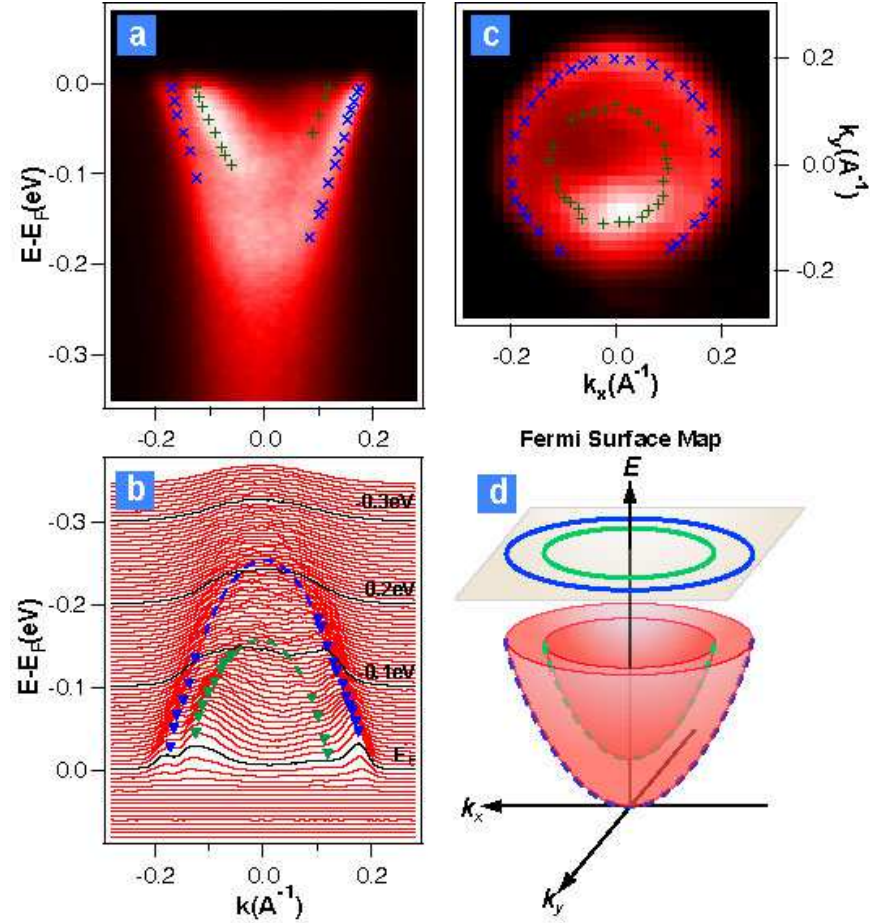


Figure 1: Observation of a surface 2DEG on SrTiO<sub>3</sub> after exposure of the cleaved (100) surface to synchrotron (UV) light. (a) ARPES data of La<sub>x</sub>Sr<sub>1-x</sub>TiO<sub>3</sub> ( $x=0.001$ ) at  $T = 20\text{K}$ , with corresponding momentum distribution curves in (b). The sample has been irradiated with  $\approx 480\text{ J/cm}^2$  UV light of 55 eV with an intensity of  $\sim 0.34\text{W/cm}^2$ . The ARPES data are taken in the second Brillouin zone using the same photon energy. The dashed lines in (b) are parabolic fits to the data points (symbols) extracted from the ARPES data; the green and blue curves have effective masses of  $\sim 0.6$  and  $0.5\ m_e$ , respectively. (c) Fermi surface map, taken on a different sample following the same preparation. Two concentric circular Fermi surface sheets (symbols) are visible. (d) shows the schematic Fermi surface and band dispersions obtained from the measured electronic structure.

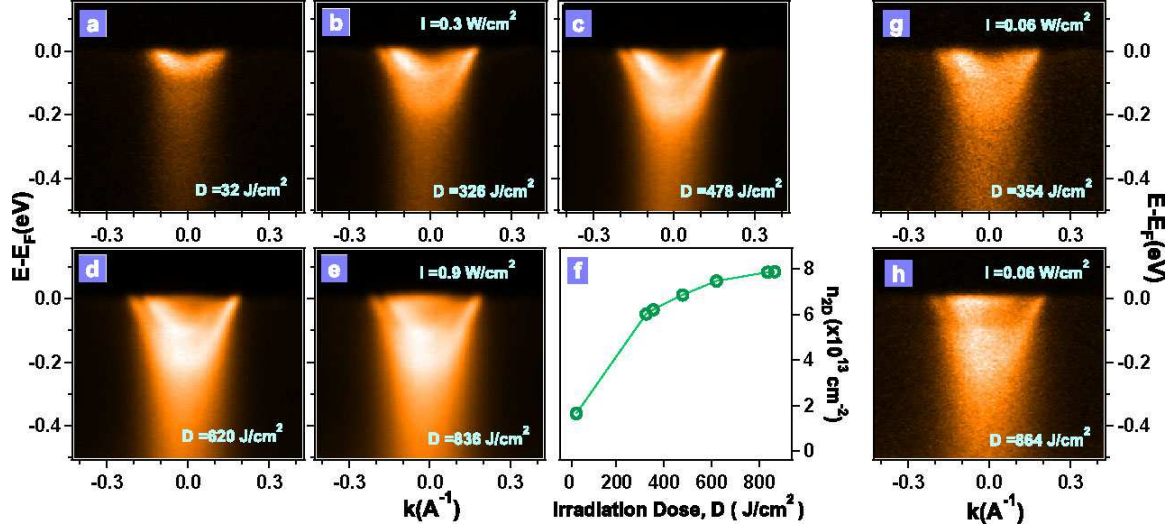


Figure 2: Variation of 2DEG charge density with exposure to different UV irradiation doses. (a)-(e), (g) and (h) show ARPES data for different irradiation doses indicated in the figure. The corresponding 2DEG charge densities as a function of irradiation dose are shown in (f). (g) and (h) show ARPES data measured immediately after (b) and (e), respectively, but with lower intensity of the probing photon beam.

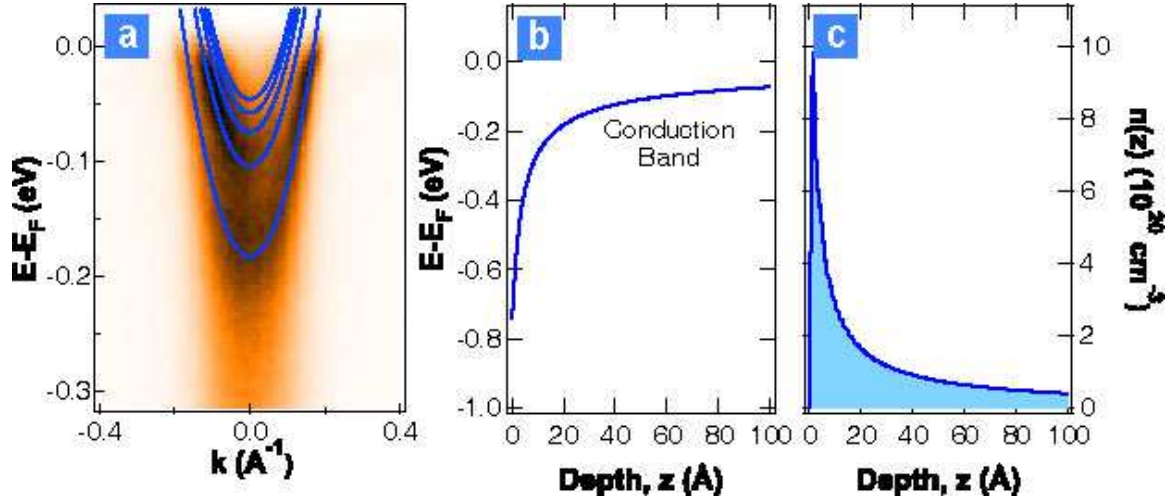


Figure 3: Calculations of quantized 2DEG states within a band-bending model [20]. (a),(b) The calculations yield quantized 2DEG states (solid lines in (a)) inside the potential well caused by the downward bending of the conduction band minimum (solid line in (b)) relative to the Fermi level, when approaching the surface of the material. The corresponding three-dimensional charge density variation as a function of depth is shown in (c). We note that in the calculation, there are three additional shallow states which are not clearly observed in the data. It is possible that these states exist in the data but are suppressed due to a combination of matrix element effects and broadening due to finite  $k_z$  dispersion of the shallow states. These considerations are supported by the observations from InAs (Fig. 4b), as well as other semiconductors [24, 25], where shallow states of a surface quantum well are more smeared out than the deeper ones.

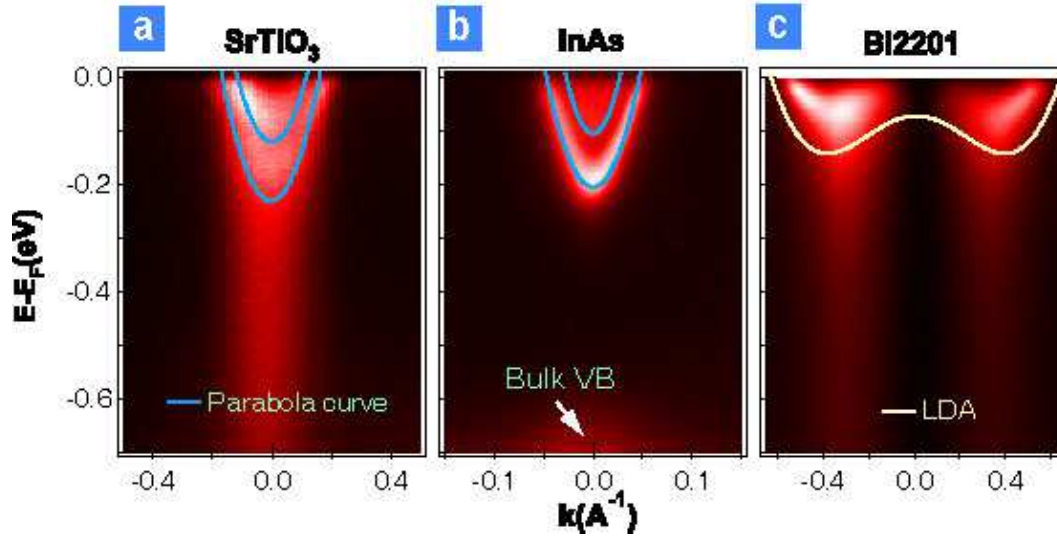


Figure 4: Comparison of ARPES data from  $\text{SrTiO}_3$ ,  $\text{InAs}$  and  $\text{Bi}_2\text{Sr}_2\text{CuO}_6$  (Bi2201) samples. (a), (b) show 2DEG states at the surface of  $\text{SrTiO}_3$  and  $\text{InAs}$ , respectively. (c) shows ARPES data from the single layer cuprate Bi2201 along  $(\pi, 0)$  to  $(0, \pi)$ . Lines in (a) and (b) are parabolic dispersion relations, to guide the eye, and the result of an LDA band-structure calculation in (c).